COMITATO NAZIONALE PER L'ENERGIA NUCLEARE
Laboratori Nazionali di Frascati

LNF-69/6
27 Gennaio 1969

W. Ash, G. Goggi, D. Grossman, G. P. Murtas, M. Nigro, G. K. O'Neill, M. Placidi, R. Santangelo, D. Scannicchio and E. Schiavuta: PROPOSAL FOR A STUDY OF BOSON PRODUCTION AT ADONE USING MAGNETIC ANALYSIS. -

Servizio Documentazione
dei Laboratori Nazionali di Frascati del CNEN
Casella Postale 70 - Frascati (Roma)

Laboratori Nazionali di Frascati del CNEN
Servizio Documentazione

LNF-69/6

Nota Interna: n. 429
27 Gennaio 1969

W. Ash(x), G. Goggi(o), D. Grossman(x), G. P. Murtas, M. Nigro(+), G. K. O'Neill(x), M. Placidi, R. Santangelo(+), D. Scannicchio(o) and E. Schiavuta(+): PROPOSAL FOR A STUDY OF BOSON PRODUCTION AT ADONE USING MAGNETIC ANALYSIS.

INTRODUCTION -

We propose to study the decay modes of 1^- (vector) mesons produced by e^+e^- annihilation in the ADONE storage ring and the production of meson resonance pairs which give a final state of bosons and photons. This program, which yields, important general information about the dynamics of the $e^+e^- \longrightarrow$ bosons interaction, is particularly well suited for the first experiments at ADONE with the planned magnetic analyser(1). Here we describe only the physics of this program, as the experimental details of measurement, accuracy etc. have been treated in a previous report(1).

(x) - Princeton University.
(o) - INFN, Gruppo di Pavia.
(+) - INFN, Sezione di Padova.

1) - PRESENT DESCRIPTION OF THE $e^+e^- \rightarrow$ BOSON PRODUCTION MECHANISM. -

Boson production by e^+e^- annihilation is currently considered as being dominated by one photon exchange.

Given the quantum numbers of the photon 1^{--} (J^{PC}), its helicity states of ± 1, and the antisymmetry of the initial wave function, one can show that of the four possible helicity states of the incident electrons, only the one combination below illustrated can contribute to the process[2]:

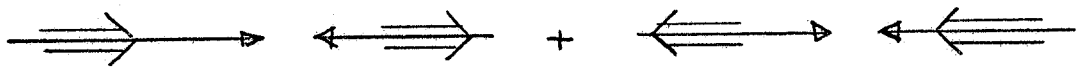

In calculating a cross section, several additional assumptions are made.

1) The vector dominance model (VDM) is used[3]. This model assumes that the electromagnetic current couples to the hadronic current only through the exchange of the appropriate combination of the vector mesons ρ^0, ω, ϕ. In the approximation that $m_\rho = m_\omega = m_\phi$, the vector meson current belongs to the octet representation of SU(3) and has zero U-spin[3,4]. The product of γ-V vertex and meson propagators are written as

$$-\frac{e}{2\gamma_\rho}\left[\frac{m_\rho^2}{K^2-m_\rho^2}\right], \quad -\frac{e}{2\gamma_\rho}\left[-\frac{\cos\theta}{\sqrt{3}}\,\frac{m_\phi^2}{K^2-m_\phi^2}\right], \quad -\frac{e}{2\gamma_\rho}\left[\frac{\sin\theta}{\sqrt{3}}\,\frac{m_\omega^2}{K^2-m_\omega^2}\right],$$

where the physical ω and ϕ have been expressed through the pure octet and singlet SU(3) states, i.e. $\phi = -\cos\theta\,\omega_8 + \sin\theta\,\omega_1$ and $\omega = \sin\theta\,\omega_8 + \cos\theta\,\omega_1$. The conventional propagator is recovered using the mixing angle: $\cos\theta = 2/3 = \cos 35^\circ$. In the calculations, the physical masses and widths are used.

Vector dominance and one photon exchange are assumed in drawing the following graph:

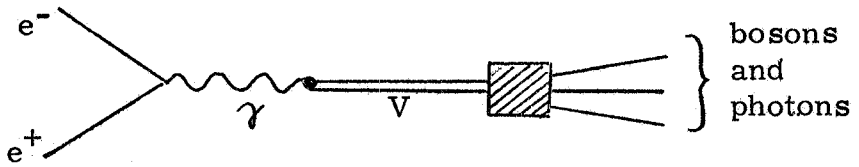

The subsequent reactions invonving the vector meson require further hypotheses for descriptions.

2) Various symmetry schemes such as SU(3), SU(6) and $SU(6)_W$ with appropriate symmetry breaking terms[5, 6] are used to describe the interactions:

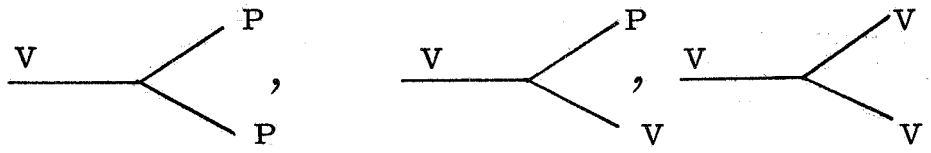

where P indicates pseudoscalar meson, and, as before, V stands for vector meson.

3) In describing the more complicated reaction

one may use crossing symmetric Regge trajectories, which involve the π-π and π-V interactions according to a model developed recently[7].

4) Finally, C conservation is assumed, in each reaction, in particular in the electromagnetic decays as

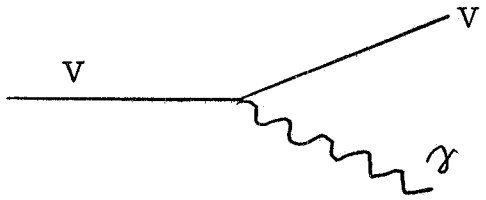

2) - HADRONIC BRANCHING RATIOS OF VECTOR MESONS -

2.1. - $\phi \to \pi^+\pi^-\pi^0$, $\pi^+\pi^-\gamma$, $\pi^+\pi^-\eta$, $K^0_S K^0_L$ etc.

Recent experimental results from ACO[8] on the branching ratios of the ϕ decay show a discrepancy from previously accepted values.

	ACO	Rosenfeld[9] 1968
$B_{K_S^0 K_L^0}$	$.308 \pm .016$	$.389 \pm .031$
$B_{K^+K^-}$	$.486 \pm .024$	$.473 \pm .032$
$B_{3\pi}$	$.206 \pm .040$	$.138 \pm .043$

Although this discrepancy will probably be resolved by other experiments before the magnet is ready for use, an experiment with magnetic analysis is essential for further investigation of the ϕ decay in several particulars.

1) Final state correlations as revealed in Dalitz plots yield information, for example, on π-π and π-ϕ interactions.

2) The presence of any $\rho^0\pi^0$ decay indicate a breaking of $SU(6)_W$ symmetry if the ω - ϕ mixing angle is given by $\cos\theta = \sqrt{2/3}$.

3) A production of $\pi^+\pi^-\gamma$ is predicted in a small percent of decays[5].

4) If C is not conserved in the electromagnetic interaction, the existence of the decay mode $\phi \rightarrow \rho^0 + \gamma$ is possible. With an assumption of maximal C violation, one expects a branching ratio of 2.4%, or equivalently $\phi \rightarrow \rho^0\gamma / \phi \rightarrow \pi^+\pi^-\pi^0 \cong 16\%$[10].

5) Having measured the branching ratio $\phi \rightarrow \pi^+\pi^-\eta$, a search for $\phi \rightarrow \rho^0\eta$, among these decays, would serve as a test of isospin conservation.

6) Finally, a study of the decay of the K_L^0 produced by the ϕ decay serves as a useful investigation of weak interaction physics. This possibility is further discussed in paragraph 9.

2.2. - $\omega \rightarrow \pi^+\pi^-\pi^0$, $\pi^+\pi^-\gamma$, etc. -

The branching ratio $\omega \rightarrow e^+e^-$ has been measured at ACO[11] as $(.79 \pm .147) \times 10^{-4}$, in disagreement with the value obtained by other methods[12], $(0.40 \pm 0.15) \times 10^{-4}$.

Although this discrepancy will probably also be resolved before the first operation of the magnet, a more accurate measurement of the production cross section and branching ratios than can be obtained without magnetic analysis, will still be needed.

Furthermore, with the magnet one can decrease the upper limit on the branching ratio $\omega \rightarrow \pi^+\pi^-\gamma$ (predicted to be 10^{-3} - 10^{-4})[5], which is now set at $\sim$ 5% with conventional techniques. Analogously to the case of the ϕ, Dalitz plot analysis on $\omega \rightarrow \pi^+\pi^-\pi^0$ yields information on the π-π and π- ω interactions[7].

3) - MESON RESONANCE PAIR PRODUCTION -

Using the assumptions previously discussed, cross sections for the productions of vector and pseudoscalar resonance pairs described by a diagram

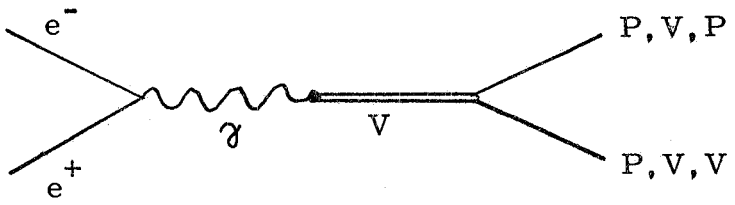

have been calculated[13]. In table I are given the predicted cross sections for an energy $W(e^+e^-) \simeq 2$. GeV, an energy at which a large number of resonance pairs should be produced with reasonable values of cross section. Although the cross sections are quite small in any case, it should still be possible to measure well those with larger cross section ($\sim 10^{-33}$ cm^2) and set a rather small upper limit on the rest. Hence the theory will be tested at high energy regarding 1) the assumption of conventional propagators for the vector mesons and energy independent form factors[3] and 2) the necessity of introducing appropriate symmetry breaking terms into the interaction.

As examples of these points, we may take the reaction $e^+e^- \rightarrow$ $\rightarrow \phi \pi^o$ and $e^+e^- \rightarrow K^{o*}\bar{K}^{o*}$. The first is forbidden by $SU(6)_W$ assuming the conventional $\omega - \phi$ mixing angle, the second by the conservation of G_U-parity (15). This last reaction is not forbidden but only strongly depressed with respect to the reaction $e^+e^- \rightarrow K^{*+}K^{*-}$ (see table I), if the physical masses and widths are used in the vector meson propagator.

4) - NEW VECTOR MESONS -

The experimental results achieved so far, do not rule out-and may even indicate-the possibility that the e. m. current must include, beside, a proper combination of ρ^o, ω , ϕ currents, some other vector meson current of presumably higher mass[14].

Furthermore, the quark model predicts a 1^- quark - antiquark $^3D_1$ state not yet observed, and the mechanism of Regge daughter trajectories, e. g. for the ρ, implies the existence of many other 1^- boson states.

If the first data from ADONE, indicate new 1^- mesons, the current description of the mechanism for $e^+e^- \rightarrow \gamma \rightarrow$ PP, PV, VV will be substantially modified, presumably giving an increase in the predicted cross sections for these reactions. For this reason it would be ex-

tremely interesting to study not only the decays of these new states, but also their influence on the production of the known bosons.

5) - EXPERIMENTAL APPARATUS -

The experimental detection apparatus, described in detail in[1] is illustrated in Figs. 1a, 1b.

External to the magnet are a series of cylindrical narrow gap chambers inter-leaved with thick plates to give γ-ray detection, range analysis, and electron-muon discrimination.

The trigger system, shown in Fig. 1c, is composed of three layers of counters, the first two between the interaction point and the spark chambers, the last outside the analysing magnet. The counter disposition and the electronic logic are chosen to allow a flexible choice of the kinds of events on which to trigger (e. g. 2 colinear charged particles, or 2 non colinear charged +1 γ-ray etc.). The charged particle trajectories are measured by a system of wide and narrow gap cylindrical and conventional spark chambers which cover $\sim$ 60% of the solid angle inside the magnetic field volume.

6) - BACKGROUND -

6.1. - Cosmic rays. -

Taking a cosmic ray flux of about 1 per cm^2 per minute per steradiant, we obtain $\sim$ 1200 counts/minute for the trigger system porposed. This number is reduced by two standard techniques.

1) Coincidence with the RF of the machine taking advantage of the fact that there are interacting particles in the interaction region only $\sim$ 10 % of the time because of beam bunching. This gives a factor of $\sim$ 10 reduction.

2) The difference in arrival time in any two diametrically opposite external counters of a cosmic ray is sufficiently different from that of an event originating from the interaction region, that the resolution of the electronic coincidence may be used to reject the cosmic rays. This time of flight technique has been tested for a geometry less ideal than ours[16] yielding a rejection factor of 20 which for our arrangement implies a rejection by $\sim$ 100. Together, than we have a rejection of $\sim$ 1000, giving $\sim$ 72 counts/hour as cosmic ray background simulating collinear events.

Cosmic ray showers which give counts even in adjacent counters, between which there is practically no time difference, act as a background when the apparatus is being triggered for non collinear events.

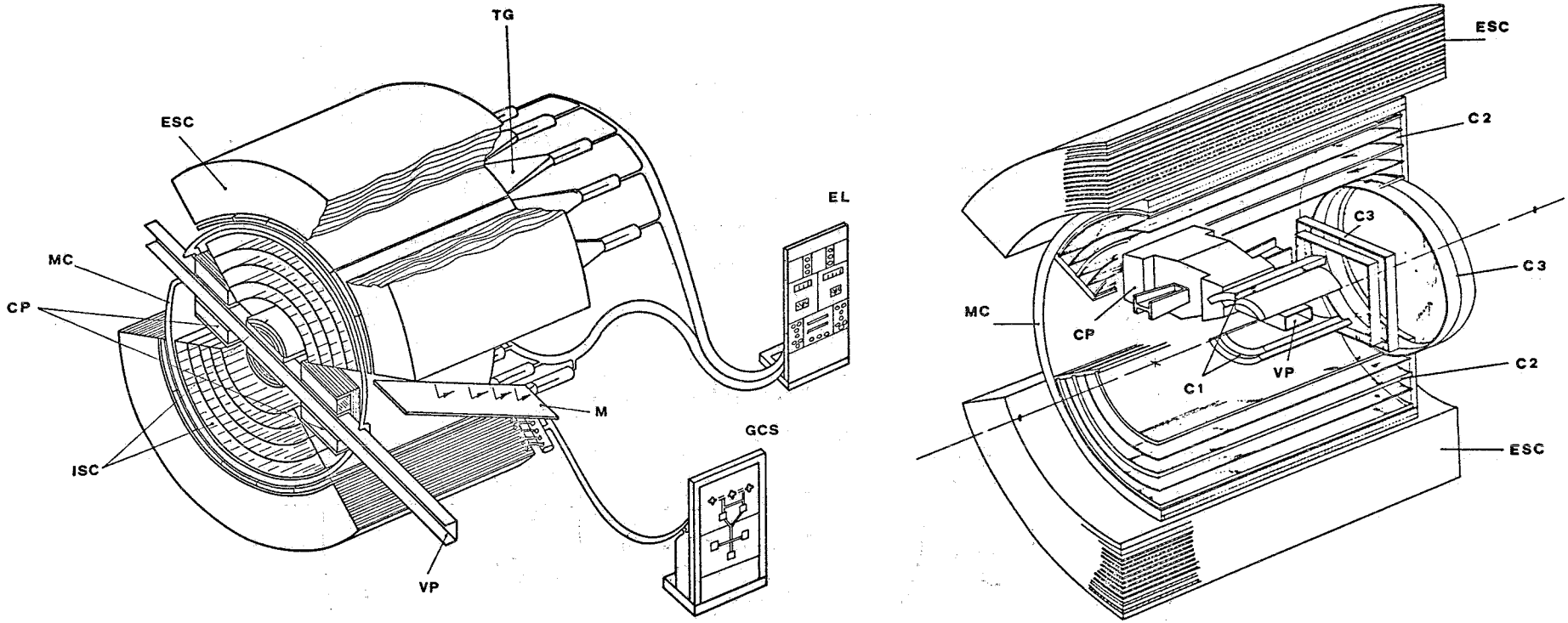

FIG. 1a, 1b - Experimental apparatus. Mc: Solenoid; VP: beam pipe; CP: magnetic field compensator; ESC: external spark chambers; ISC: internal spark chambers; C1, C2: cylindrical wire spark chambers; C3: wire plane chamber; GCS: Gas control system; M: mirror; TG: trigger external counter; EL: electronic logic.

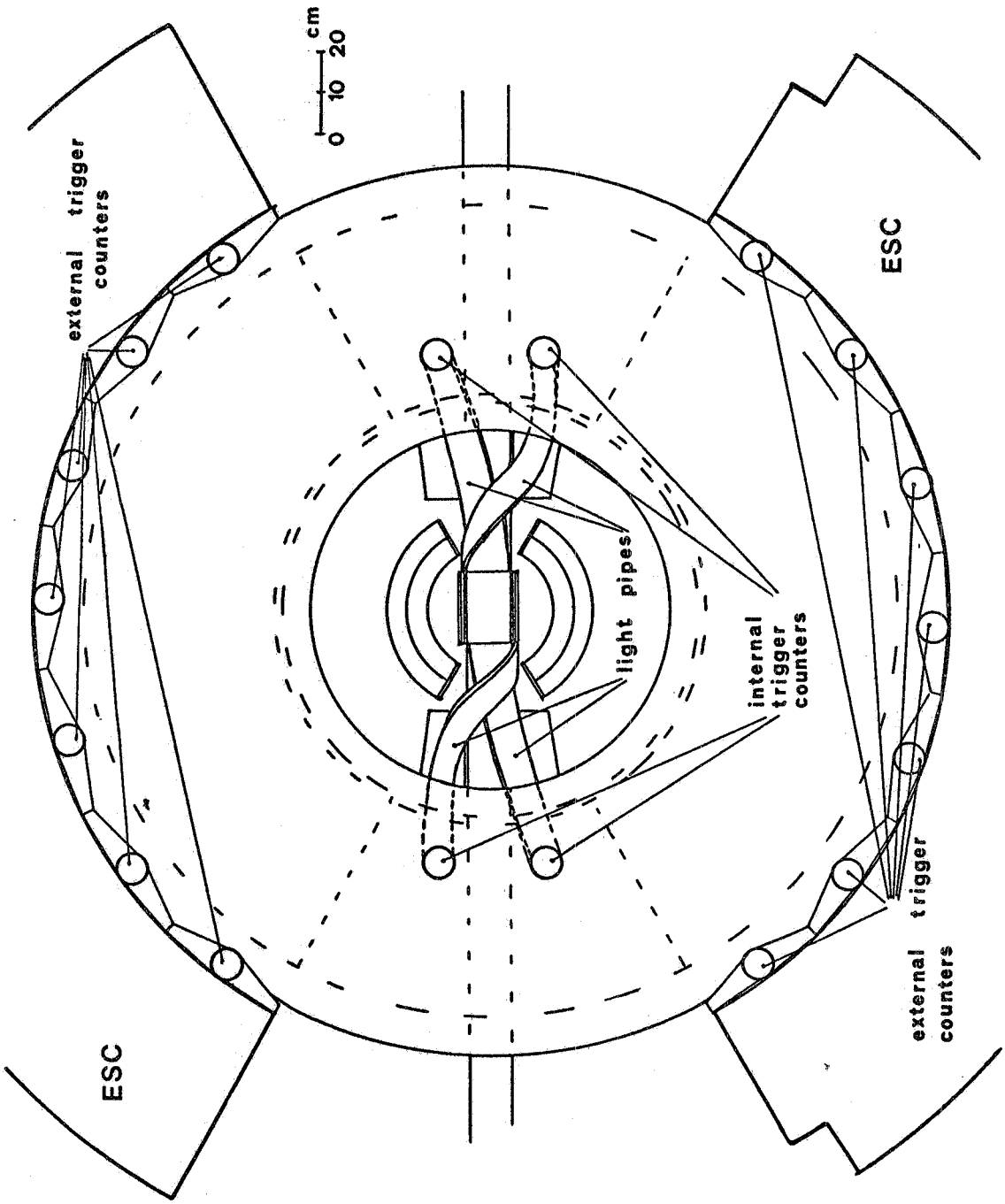

FIG. 1c - Trigger system.

This background, however, can be largely reduced by employing as anti-coincidence extra counters which cover solid angle not presently being used.

6.2. - Machine Background. -

Scattering of the beam from residual gas, or vacuum pipe walls constitutes a non trivial source of counts which simulate events. During early tests of ADONE, several measurements were made of this process for varying geometries, counter logic, and vacuum[17]. From these measurements we have extracted rough estimates of the background for our apparatus.

An apparatus with a similar trigger arrangement in the horizontal plane gives ~ 15 triggers per milliampere of beam current lost.

A typical mean beam loss of ~ 10 mA per hour per beam gives ~ 300 counts per hour.

A second test indicated that the background decreases away from the median plane. This effect and a correction for solid angle reduce the expected rate for our apparatus by a factor 1.5.

We expect a further reduction caused by rejection of low energy particles by action of the magnetic field. This effect is estimated at about 5 by comparing test data with different coincidence levels. In all we expect ~ 40 triggers/hour from the machine. This could be further reduced by ~ 10 introducing shielding, already provided in part by the bulk of the compensators and magnet coil, to avoid background originating outside the interaction region.

7) - PRODUCTION AND DECAY OF THE ϕ. -

7.1. - $e^+e^- \rightarrow \phi \rightarrow \pi^+\pi^-\pi^o$, $\pi^+\pi^-\gamma$.

a) Detection Efficiency and Resolution.

In order to study the efficiency and resolution of the apparatus we simulated events of the following kind with a Monte Carlo program[18].

$$e^+e^- \rightarrow \pi^+\pi^-\gamma \qquad \text{(A)}$$

$$\rightarrow \rho\pi \rightarrow \pi^+\pi^-\pi^o \qquad \text{(B)}$$

$$\rightarrow \pi^+\pi^-\eta \qquad \text{(D)}$$

The events of type (A) and (D) were created assuming a phase-space distribution. The events of type (B) were created, instead, assuming the mechanism $e^+e^- \rightarrow \rho^+\pi^- + \rho^o\,\pi^o + \rho^-\pi^+ \rightarrow \pi^+\pi^-\pi^o$. However the conclusions do not change appreciably if a phase-space me-

chanism is assumed.

The program assumed values for precision of measurements which have been previously calculated for this apparatus[1]. For the $\pi^+\pi^-$ pairs, account was further taken of the loss at the low momenta due to nuclear interaction in the magnet coil, as well as of the dynamics of production[2].

The results are summarized in table II. In particular we note that the detection efficiencies for events in which a photon of energy K_γ greater then 100 MeV is detected in addition to the π^+ and π^- (in the case of a π^o, the photon is one of the decay γ's) are

$$\text{(A)} \quad \bar{\varepsilon}_\gamma(\pi^+\pi^-\gamma) = 0.08$$

$$\text{(B)} \quad \bar{\varepsilon}_\gamma(\pi^+\pi^-\pi^o) = 0.052$$

The missing mass distribution of the $\pi^+\pi^-$ system for these two cases is given in Fig. 2. Fig. 3 gives the same distribution for the case without γ detection.

Although there is a small advantage in detecting also the γ in reaction (B), a clear distinction between (A) and (B) is not possible on this basis alone as the reaction rate of (A) is expected to be only a few percent that of (B)[5].

Selecting only events with $MM^2 \leq 0$, the two detection efficiencies become (see table II):

$$\text{(A)} \quad \bar{\varepsilon}'_\gamma(\pi^+\pi^-\gamma) = 0.04$$

$$\text{(B)} \quad \bar{\varepsilon}'_\gamma(\pi^+\pi^-\pi^o) = 0.0065$$

The apparatus in this case is six times more sensitive to (A) than (B).

b) Angular Distribution of the Detected Photon. -

A further separation of events of type (A) from those of (B) can be made by measuring the angle $\theta_{\gamma N}$ between the photon and the missing neutral. For reaction (A), one must have a distribution with a maximum for $\theta_{\gamma N} \sim 0^o$ whereas in the case of (B) $\theta_{\gamma N}$ will be characteristic of the π^o decay.

These distributions, also obtained from the Monte Carlo program are shown in Fig. 4 assuming a ratio $\phi \to \pi^+\pi^-\gamma / \phi \to \rho\pi \to \pi^+\pi^-\pi^o$ of .02, and 10^5 events of type (B). The cut at $\theta_{\gamma N} \simeq 40^o$ for case (B) is caused by the cut assumed for the photon energy, $K_\gamma > 100$ MeV.

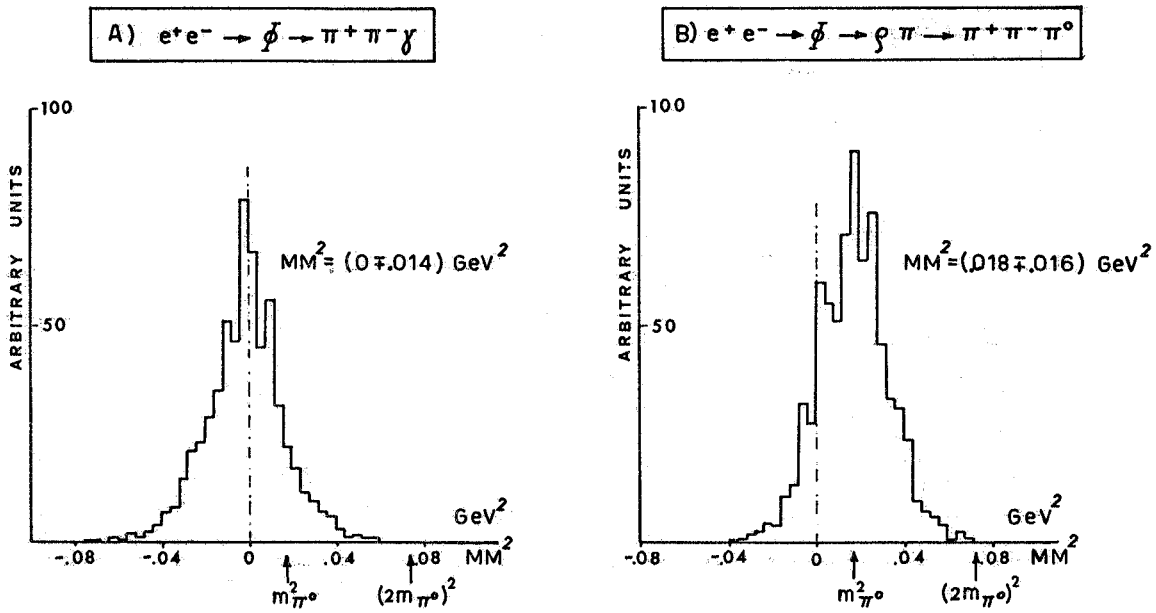

FIG. 2 - Missing mass of the charged particles (events with π^+,π^- and only one γ of energy 0.1 GeV are considered).

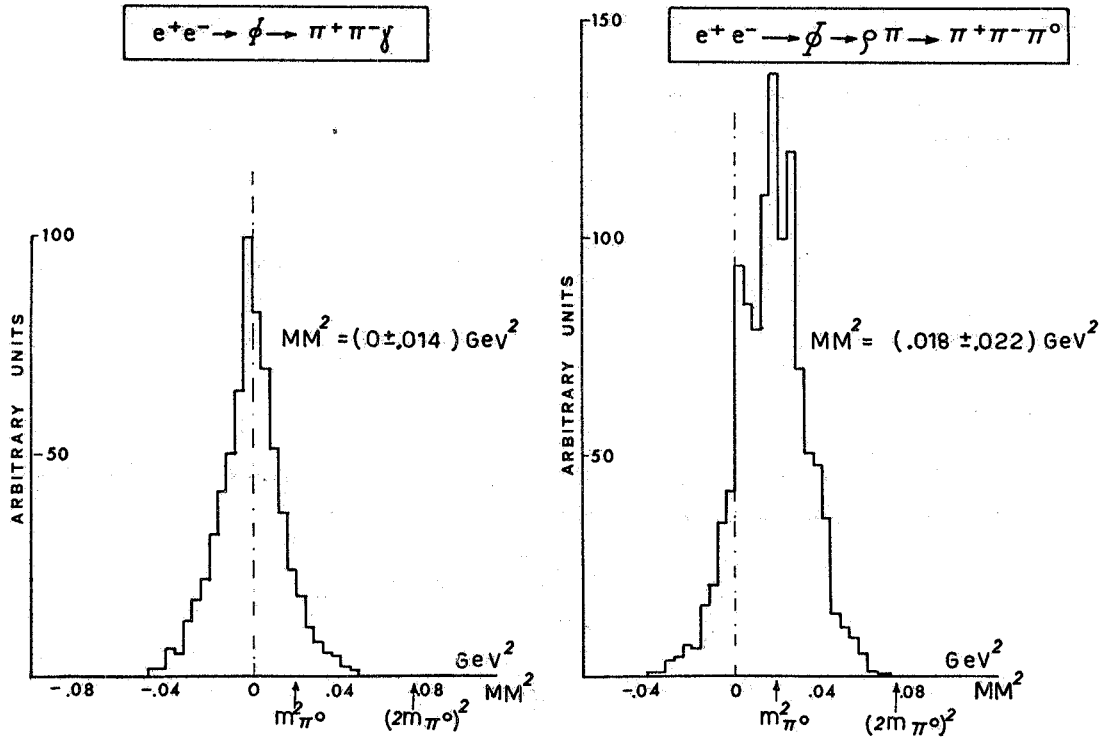

FIG. 3 - Missing mass of the charged particles (π^+, π^- are detected but γ detection is not required).

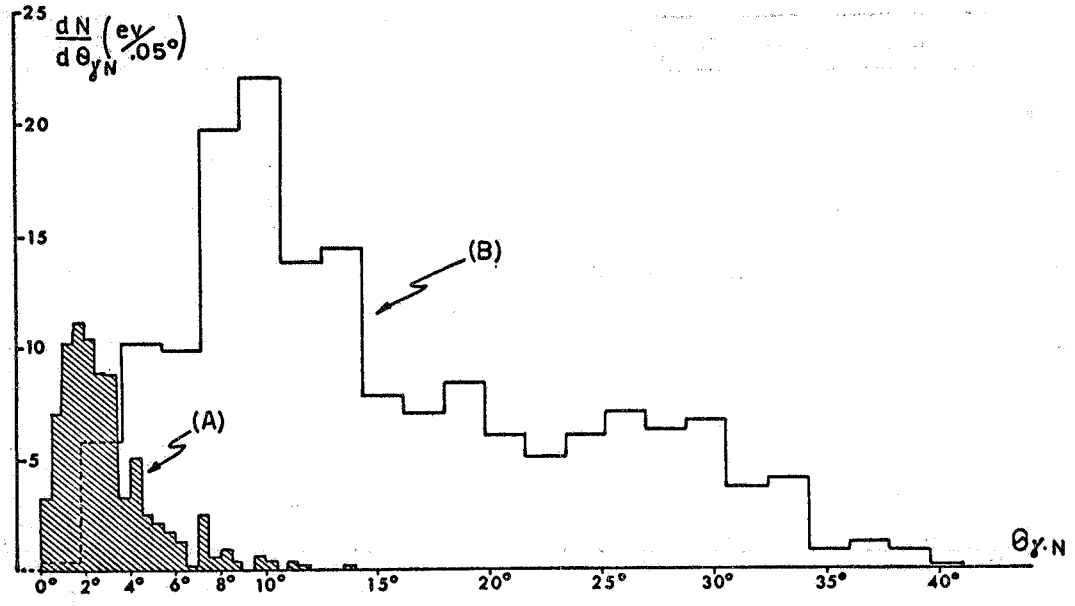

FIG. 4 - Distribution of the angle $\theta_{\gamma N}$ between the γ and the missing neutral (events with $\pi^+\pi^-$ and only one γ of energy > 0.1 GeV, with the further condition $MM^2 \leq 0.0$, are considered).
After the previous conditions, 81 events survive from the 2.10^3 initial $e^+e^- \rightarrow \phi \rightarrow \pi^+\pi^-\gamma$ produced reactions, and 650 events survive from the 10^5 initial $e^+e^- \rightarrow \phi \rightarrow \rho\pi \rightarrow \pi^+\pi^-\pi^o$ produced reactions.

Selecting now events with $\theta_{\gamma N}$ between 0^o and 2^o, $MM^2 \leq 0$, and assuming that reaction (A) is 2% as frequent as (B), we obtain (see table II):

$$\frac{\text{number of (A) events}}{\text{number of (B) events}} \simeq \frac{0.02 \times .16 \times 10^{-1}}{.038\ 10^{-3}} \simeq 8;$$

i. e. a contamination of 12%.

c) Running Time. -

Using the same assumptions as above, we have for the number of detected events of type (A) and (B) (see table II):

$$N_A = 16 \times 10^{-5}\ \eta_{\pi\pi\gamma} N$$
$$N_B = 3.8 \times 10^{-5}\ N$$
$$N_T = N_A + N_B$$

where N equals the total number of events of type (B) produced and

$$\eta_{\pi\pi\gamma} = \frac{\phi \rightarrow \pi^+\pi^-\gamma}{\phi \rightarrow \rho\pi \rightarrow \pi^+\pi^-\pi^o} \text{ (in \%)}$$

By taking only those events with $\theta_{\gamma N} \geq 4^o$, and the predicted Monte Carlo distribution it is possible to extrapolate the $\rho\pi$ background into the region of interest ($\theta_{\gamma N} < 2^o$) and extract the value of N_B.

We define a parameter $K = (N_T - N_B)/\sqrt{N_T}$ as the number of standard deviations by which the measured number of events of type (A) exceed the contamination from those of (B).

This is plotted as a function of N in Fig. 5a. The requirement that K exceed 3σ implies a total number of events equal to $4 \cdot 10^4$ if the branching ratio ($\phi \to \pi^+\pi^-\gamma / \phi \to \rho\pi \to \pi^+\pi^-\pi^o$) = .02.

We may now calculate the expected event rate and the required running time to yield the above number of 40,000 $e^+e^- \to \phi \to \pi^+\pi^-\pi^o$ events.

Using the nominal ADONE luminosity[19] at the ϕ energy, L = $= .375 \times 10^{33}$ cm^{-2} hr^{-1}, and the peak cross-section value measured at ACO[8] we have

$$\bar{N} = L\sigma\varepsilon(\pi^+\pi^-) = 0,375 \cdot 10^{33} \cdot 0,74 \cdot 10^{-30} \times 0,16 = 44(\pi^+\pi^-)/\text{hour}$$

Working at seven different energy values to measure the ϕ production without ambiguity and to extract the ϕ width, one arrives at a required running time of 220 hours, as reported in table IV. Assuming instead $\phi \to \pi\pi\gamma / \phi \to \rho\pi \to \pi^+\pi^-\pi^o = 0.01$ the events collected in 330 hours correspond to K = 2.7 standard deviations.

7.2. - $e^+e^- \to \phi \to \rho^o\gamma$ (reaction (C)).

In studying this decay, one selects those events in which the invariant mass of the two charged particles lies in the range $(m_\rho - \Gamma_\rho)^2 \leq$ $\leq M^2_{\pi^+\pi^-} \leq (m_\rho + \Gamma_\rho)^2$. Using the Monte Carlo program, we have estimated the contamination from events of (A) and (B). With a total number of interactions of type $e^+e^- \to \rho\pi \to \pi^+\pi^-\pi^o$ equal to 4×10^4, we have (tables II and III):

$\bar{N}_A$ = 1.6 (events $\pi^+\pi^-\gamma$ of $\pi^+\pi^-\gamma$ reaction)
with $(m_\rho - \Gamma_\rho)^2 \leq M^2(\pi^+\pi^-) \leq (m_\rho + \Gamma_\rho)^2$

$\bar{N}_B$ = .6 (events $\pi^+\pi^-\gamma$ of $\rho\pi^o$ reaction)
with $(m_\rho - \Gamma_\rho)^2 \leq M^2(\pi^+\pi^-) \leq (m_\rho + \Gamma_\rho)^2$

assuming a ratio $\eta_{\pi\pi\gamma} = (\phi \to \pi\pi\gamma / \phi \to \rho\pi \to \pi^+\pi^-\pi^o) = 0.01$ and the mass range mentioned above.

If $\eta_{\rho\gamma} = \phi \to \rho\gamma / \phi \to \rho\pi \to \pi^+\pi^-\pi^o = 0.01$, the number of genuine events is $\bar{N}_C$ = 6.3 (events $\pi^+\pi^-\gamma$ of $\rho^o\gamma$ reaction) with $(m_\rho - \Gamma_\rho)^2 \leq$

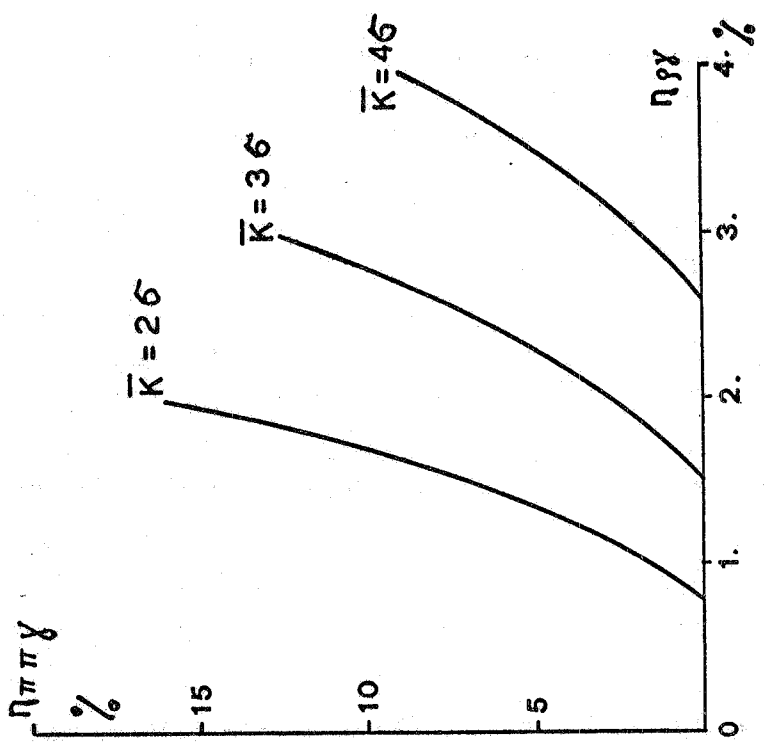

FIG. 5b - Separation of reaction $e^+e^- \to \phi \to \rho\pi \to \pi^+\pi^-\pi^0$ and $e^+e^- \to \phi \to \pi^+\pi^-\gamma$ in units of standard deviation σ (see text, § 7.2) as a function of

$$\eta_{\pi\pi\gamma} = \frac{\phi \to \pi^+\pi^-\gamma}{\phi \to \rho\pi \to \pi^+\pi^-\pi^0},$$

$$\eta_{\rho\gamma} = \frac{\phi \to \rho\gamma}{\phi \to \rho\pi \to \pi^+\pi^-\pi^0} \text{ (in \%)}$$

For $N = 4 \cdot 10^4$.

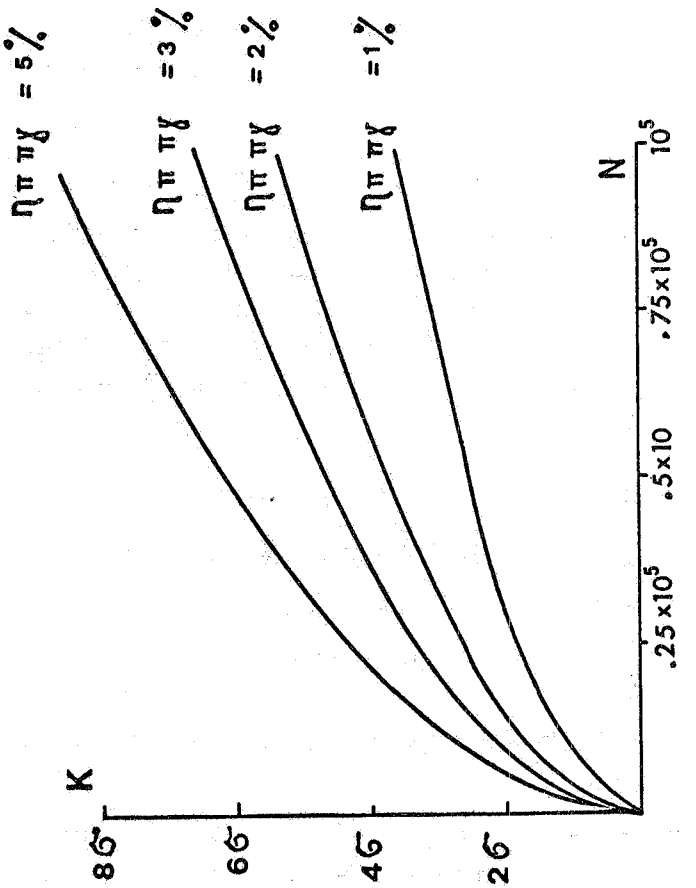

FIG. 5a - Separation of reaction $e^+e^- \to \phi \to \rho\pi \to \pi^+\pi^-\pi^0$) in units of standard deviation σ (see text, § 7.1) as a function of the produced events N, $e^+e^- \to \phi \to \rho\pi \to \pi^+\pi^-\pi^0$), for different values of

$$\eta_{\pi\pi\gamma} = \frac{\phi \to \pi^+\pi^-\gamma}{\phi \to \rho\pi \to \pi^+\pi^-\pi^0} \text{ (in \%)}$$

$\leq M^2(\pi^+\pi^-) \leq (m_\rho + \Gamma_\rho)^2$.

In order to separate $\bar{N}_C$ from $\bar{N}_A + \bar{N}_B$, we extrapolate the $\bar{N}_A + \bar{N}_B$ background into the region of interest ($(m_\rho - \Gamma_\rho)^2 \leq M^2(\pi^+\pi^-) \leq (m_\rho + \Gamma_\rho)^2$), using a method indicated to be satisfactory by the Monte Carlo results.

The parameter

$$\bar{K} = \frac{\bar{N}_T - (\bar{N}_B + \bar{N}_A)}{\sqrt{\bar{N}_T}}$$

analogous to K, gives the number of standard deviations by which the measured events in this mass range stand above the extrapolated background from (A) and (B). In Fig. 5b are shown the values of the branching ratios $\eta_{\rho\gamma}$ and $\eta_{\pi\pi\gamma}$ for which $\bar{K}$ = 2, 3 and 4 standard deviations, assuming a total number of $\rho\pi$ produced reactions equal to 4×10^4.

7.3. - $e^+e^- \rightarrow \phi \rightarrow \pi^+\pi^-\eta$, Reaction (D).

a) The separation of these events from those of (B) is possible only on the basis of a measurement of missing mass of the charged particles.

In Fig. 6, we give the two distributions in MM^2 for reactions (B) and (D) in which the only requirement is the detection of the $\pi^-\pi^+$ pair.

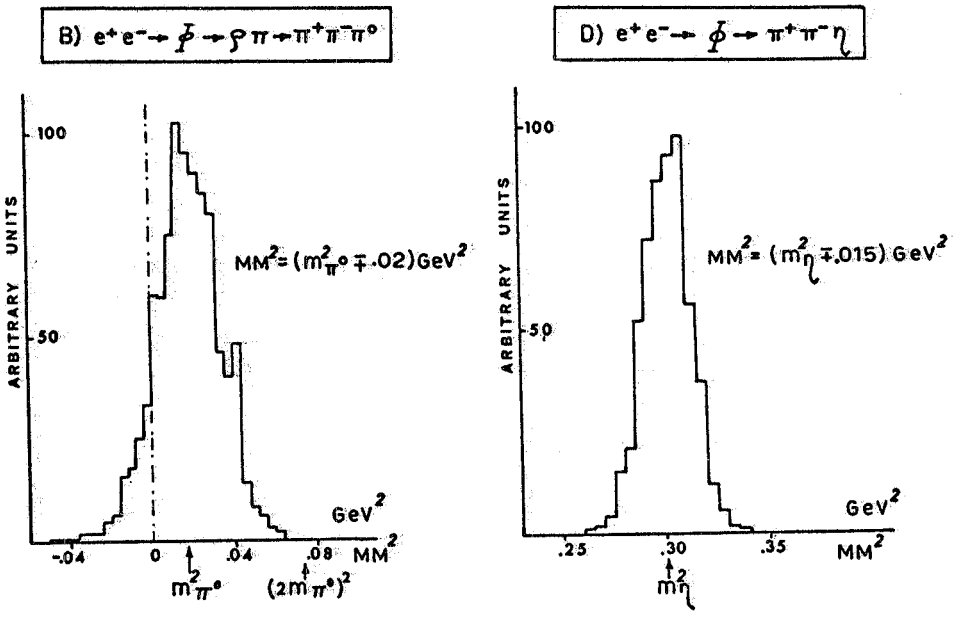

FIG. 6 - Missing mass of the charged particles (π^+, π^- are detected but γ detection is not required).

In table V is given the detection efficiency of the $\pi^+\pi^-$ pair obtained by the Monte Carlo program assuming a total number of $\phi \rightarrow \rho\pi$

events of 4 x 10^4. From this, it appears that one ought to be able to measure the ratio $\phi \rightarrow \pi^+\pi^-\eta / \phi \rightarrow \pi^+\pi^-\pi^o$ to below 1 percent.

b) if all the products of this reaction are observed, i. e. also the γ's from η decay, a further separation of (B) from (D) can be made on the basis of the γ's opening angle. In Fig. 7 is shown the distribution in opening angle of the decay γ's from reaction (B); combining this information with the opening angle of γ decay from the η ($\theta_{\gamma\gamma} \simeq 92^o$),

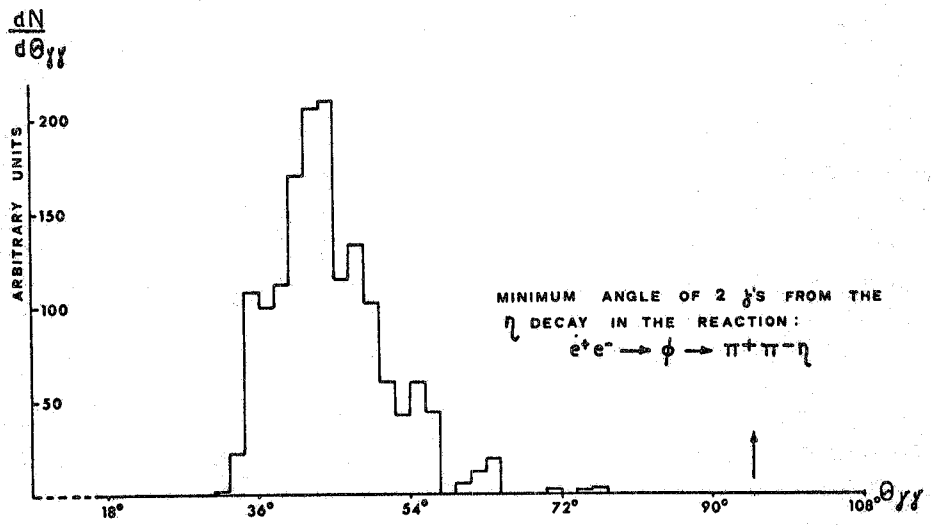

FIG. 7 - Distribution of the $\theta_{\gamma\gamma}$ angle between the two γ's from the π^o decay, for events $e^+e^- \rightarrow \phi \rightarrow \rho\pi \rightarrow \pi^+\pi^-\pi^o$ (events with $\pi^+\pi^-$ and both γ's with energy > 0.1 GeV are considered).

the separation seems quite well defined. The detection efficiency in this case has been evaluated and is shown in table V.

7.4. - Dalitz Plot.

With the 6400 events in which the charged particles are detected one can accurately study the Dalitz plot $e^+e^- \rightarrow \phi \rightarrow \pi^+\pi^-\pi^o$, in particular determining the ratio $\phi \rightarrow \rho\pi / \phi \rightarrow \pi^+\pi^-\pi^o$ to high precision. In order to make an accurate analysis of this plot, however, one must know how reliable are the corrections due to the geometrical and kinematical cuts introduced by the apparatus. In Fig. 8 is given the distribution in the angle θ between the normal of the production plane with the beam direction as predicted by the Monte Carlo program. From a theoretical point of view, one predicts a distribution in $\sin^2\theta^{(2)}$ on general grounds. The exact knowledge of the distribution in θ, then, shall permit to estimate the reliability of the Monte Carlo calculations. In fact, the experimental distribution in θ must equal that predicted by the program, if the calculations are to be trusted in further analysis.

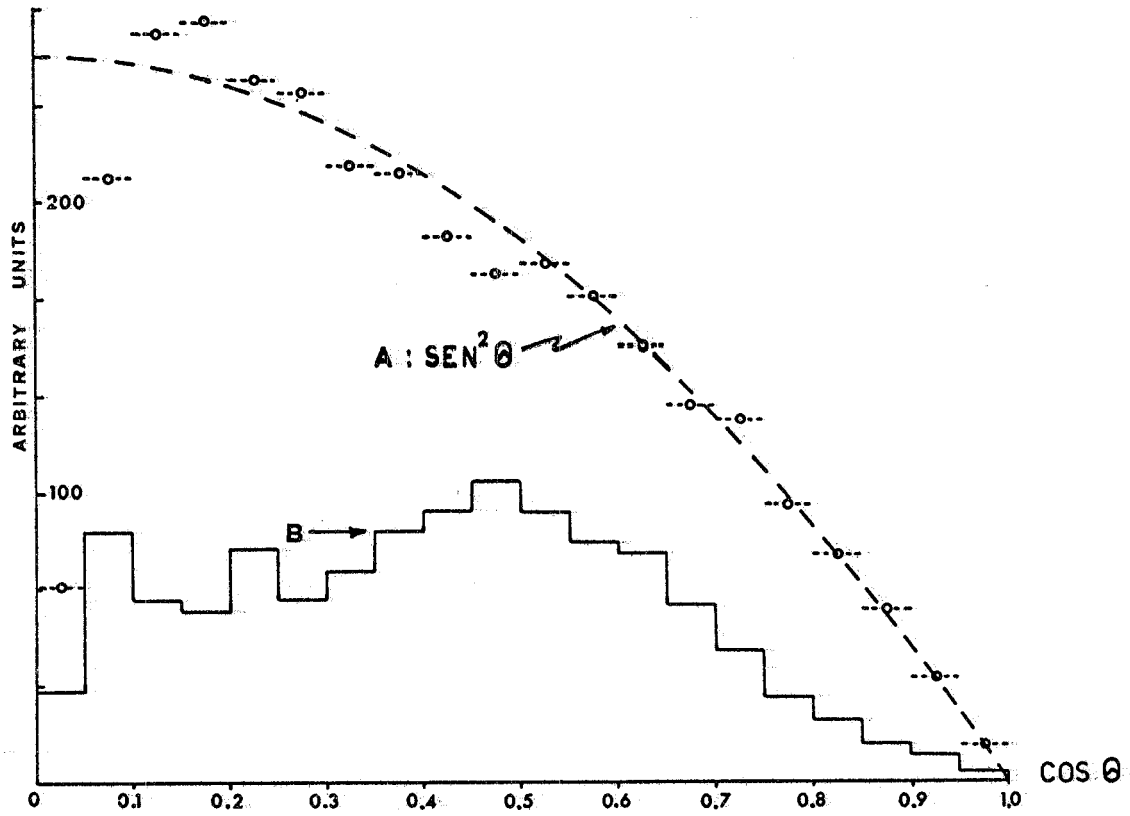

FIG. 8 - Distribution of θ , angle between the normal to the reaction plane ($\pi^+\pi^-\pi^o$) and the (e^+e^-) beam direction for the reaction $e^+e^- \rightarrow$ $\rightarrow \phi \rightarrow \rho\pi \rightarrow \pi^+\pi^-\pi^o$.
A: theoretical distribution. B: expected experimental distribution (π^+ and π^- are detected but γ detection is not required).

8) - ω PRODUCTION AND DECAY -

The cross section of the process $e^+e^- \rightarrow \omega \rightarrow \pi^+\pi^-\pi^o$ is at least a factor 2 greater than that of $e^+e^- \rightarrow \phi \rightarrow \pi^+\pi^-\pi^o$(8), while the luminosity of the machine at the ω energy is about 30% less than that of the ϕ. In 120 hours, than , one should be able to obtain information analogous to that already discussed for the ϕ by analysing the Dalitz plot of $\omega \rightarrow \pi^+\pi^-\pi^o$. Further, one can set a limit of 1-2% on the branching ratio ($\omega \rightarrow \pi^+\pi^-\gamma$)/($\omega \rightarrow \pi^+\pi^-\pi^o$).

9) - $e^+e^- \rightarrow$ V + V, V + P, P + P. -

For certain reactions of table I, we have evaluated the counting rate as given in table VI. While in the ϕ and ω reactions previously discussed, the full available solid angle of the magnet (i. e. including the

axial spark chambers C_3 of Fig. 1) is not necessary and has not been assumed, the multibody cross sections are sufficiently low to demand the use of the extra chambers. The efficiencies of table VI include this modification.

In 300 hours, it should be possible to measure the cross sections of reaction 1, 2, 4 and 5 of table VI, and to put a reasonable upper limit on the cross section for $K^{*+}K^{*-}$ production.

The detection efficiencies for the various decay channels of these reactions are currently being studied using Monte Carlo techniques.

10) - STUDY OF THE K_L^o DECAY -

The K_L^o K_S^o decay of the ϕ in the experimental apparatus offers unique advantages in studying the K_L^o decay modes[20]. The $\pi^+\pi^-$ decay of the K_S^o serves as an unambiguous measure of the flux of K_L^o produced. The requirement of extrapolating the tracks of the decay products of the K_L^o to a point outside the interaction region but in a plane defined by the K_S^o decay results in negligible background for this process.

Consequently, one can measure the absolute branching ratios of the K_L^o to a higher precision than yet obtained, eliminating the ambiguity that exists to date on the $3\pi^o$ branching ratio. Furthermore, an accurate measure of the momentum spectra in the leptonic decays would provide information necessary for an evaluation of the coupling involved in this reaction and of the form factors. Finally, given above nominal luminosity for ADONE, there would be enough 2π decays of the K_L^o to give strong conclusions about the unresolved CP violation mechanism.

The expect yield, of a 400 hour run, in the various decay modes has been calculated assuming conservative detection efficiencies, the peak ϕ cross section measured at ACO (accounting for radiation effects), and the design luminosity of ADONE, with results tabulated below (table VII). Calculations of background and of the precision of momentum spectra measurements obtainable given the resolution of the magnet and its π, μ, e discrimination are in progress.

REFERENCES -

(1) - W. Ash, D. Grossman, G. Matthiae, G. P. Murtas, M. Nigro, G. K. O'Neill, G. Sacerdoti, R. Santangelo, D. Scannicchio and E. Schiavuta, A magnetic analyzer to be used for Adone colliding beam experiments, LNF-69/2 (1969).

(2) - S. De Gennaro, E. Celeghini, G. Longhi and R. Gatto, Nuovo Cimento 47, 113 (1967); N. Cabibbo and R. Gatto, Phys. Rev. 124, 1577 (1961).

(3) - N. M. Kroll, T. D. Lee and B. Zumino, Phys. Rev. 157, 1876 (1967).

(4) - H. Joos, Vector mesons and the electromagnetic interactions of hadrons, DESY 67/13 (1967).

(5) - J. Yellin, Phys. Rev. 147, 1080 (1966).

(6) - L. M. Brown, H. Munczek and P. Singer, Phys. Rev. Letter 21 707 (1968).

(7) - G. Veneziano, Nuovo Cimento 57A, 190 (1968).

(8) - J. E. Augustin, J. C. Bizot, J. Buon, B. Delcourt, J. Haissinski, J. Jeanjean, D. Lalanue, P. C. Marin, H. Nguyen Ngoc, J. Perez--Jorba, F. Richard, E. Rumpf and D. Treille, Comunication at XIV International Conference on High Energy Physics (Vienna, 1968).

(9) - A. H. Rosenfeld et al., Tables U. C. R. L. (Agosto, 1968).

(10) - J. Bernstein, G. Feinberg and T. D. Lee, Phys. Rev. 139, B 1650 (1965).

(11) - J. E. Augustin, D. Benaksas, J. Buon, V. Gracco, J. Haissinski, D. Lalanue, F. Laplanche, J. Lefrancois, P. Lehmann, P. Marin, F. Rumpf and E. Silva, Communication at XIV International Conference on High Energy Physics (Vienna, 1968).

(12) - D. Bollini, A. Buhler, P. Dalpiaz, T. Massam, F. Navach, F. L. Navarria, N. A. Schneegaus and A. Zichichi, Nuovo Cimento 57, A 404 (1968).

(13) - Shui-Yin-Lo, Phys. Rev. 148, 1431 (1966).

(14) - E. Celeghini, R. Gatto, Meson resonances from Electron-Positron Colliding Beams. Internal Report TH 68-2, Istituto di Fisica, Firenze.

(15) - R. Santangelo, Nuovo Cimento 56, A 1129 (1968).

(16) - L. Paoluzi, R. Visentin, Nuclear Instr. and Meth. 65, 345 (1968).

(17) - F. Palmonari, Nota Interna of LNF to be published.

(18) - Programming work was performed by M. Locci and M. A. Mencuccini Spano. A detailed description of the program will be published.

(19) - F. Amman, Dimensioni dei fasci, vite medie, luminosità e caratteristiche della zona di interazione di Adone, LNF-66/6 (1966).

(20) - G. K. O'Neill, The study of the K^o meson decays by colliding beams LNF-68/43 (1968).

TABLE I

	Reaction	$\sigma(cm^2)$	Decay channels
$e^+e^- \to \gamma \to V+V$	$\rho^+\rho^-$	10^{-33}	
	$K^{*+}K^{*-}$	5.10^{-33}	$\frac{16}{81}$ in $K^\circ(\pi^+\pi^-)\pi^+\bar{K}^\circ(\pi^+\pi^-)\pi^-$ $\frac{4}{27}$ in $K^\circ(\pi^+\pi^-)\pi^+K^-\pi^\circ$ $\frac{4}{27}$ in $K^+\pi^\circ\bar{K}^\circ(\pi^+\pi^-)\pi^-$
	$K^{*\circ}\bar{K}^{*\circ}$	3.10^{-34}	$\frac{4}{27}$ in $\bar{K}^\circ(\pi^+\pi^-)\pi^\circ K^+\pi^-$ $\frac{4}{27}$ in $K^-\pi^+K^\circ(\pi^+\pi^-)\pi^\circ$ $\frac{4}{9}$ $K^-\pi^+K^+\pi^-$
$e^+e^- \to \gamma \to P+P$	$\pi^+\pi^-$	10^{-34}	
	K^+K^-	10^{-34}	
	K_1K_2	10^{-35}	
$e^+e^- \to \gamma \to V+P$	$\rho^\circ\pi^\circ$	8.10^{-34}	
	$\rho^\circ\eta$	10^{-33}	
	$\omega\eta$	10^{-34}	
	$K^{*+}K^-$	10^{-36}	$\frac{1}{3}$ $K^+\pi^\circ K^-$, $\frac{1}{9}$ in $K^\circ(\pi^+\pi^-)\pi^+K^-$
	$\omega\pi^\circ$	6.10^{-33}	
	$\bar{K}^{*\circ}K^\circ$	3.10^{-33}	$\frac{4}{27}$ in $\bar{K}^\circ(\pi^+\pi^-)\pi^\circ K^\circ(\pi^+\pi^-)$ $\frac{4}{9}$ in $K^-\pi^+K^\circ(\pi^+\pi^-)$
	$\rho^\circ\eta'$	6.10^{-34}	
	$\phi\eta'$	10^{-34}	
	$\omega\eta'$	8.10^{-35}	
	$\phi\eta$	2.10^{-35}	
	$\phi\pi^\circ$	0	mixing angle between ω-ϕ assumed to be 35°.

TABLE II

Reactions: (A): $e^+e^- \rightarrow \pi^+\pi^-\gamma$; (B): $e^+e^- \rightarrow \rho\pi \rightarrow \pi^+\pi^-\pi^o$

Event type	Detection efficiency		(A)	(B)
1	Percentage of detected $\pi^+\pi^-$ (a), (b)	ε	.2	.16
2	Percentage of detected $\pi^+\pi^-$ with only one γ of energy >0.1 GeV (a), (b)	ε_γ	.1	.065
3	Percentage of events of type 2 with the further condition: $MM^2<0.0$ (see text) (a), (b)	ε'_γ	.05	.008
4	Percentage of events of type 2; γ detection efficiency as in (c)	$\bar{\varepsilon}_\gamma$	.08	.052
5	Percentage of events of type 3; γ detection efficiency as in (c)	$\bar{\varepsilon}'_\gamma$	.04	.0065
6	Percentage of events of type 5, having $\phi_{\gamma N}$ (angle γ-missing neutral) between 0°-2°	$\bar{\varepsilon}_\phi$	$.16\times10^{-1}$	$.038\times10^{-3}$
7	Percentage of events of type 6; with the condition ($0.42\leq \leq m^2(\pi^+\pi^-)\leq 0.76$) i.e. in the $(m_\rho \pm \Gamma_\rho)$ interval	$\bar{\varepsilon}_\rho$	$.04\times10^{-1}$	$.013\times10^{-3}$

(a) efficiency of the experimental apparatus (counters and spark chambers) assumed to be 1;
(b) the losses due to nuclear interactions and range in the coil, are included;
(c) γ detection efficiency in the external chambers is assumed to be 0.8 (1) (shower electrons are visible at least in 3 bigaps).

TABLE III

Number of events $e^+e^- \to \rho\pi$ produced	40.000
Number of events $e^+e^- \to \rho\pi$ with $\pi^+\pi^-$ detected ($\varepsilon(\rho\pi)=\cdot 16$)	6.400
Number of events (π^+,π^- and only one γ of energy >0.1 GeV are detected) $\bar{\varepsilon}_\gamma = 0.052$	2.080

TABLE IV

Energy	$\sigma(E)/\sigma(m_\phi)$	Events/hr	Events	Hours
m_ϕ	1	43.6	3400	77.8
1.0215	0.64	27.9	1000	35.8
1.0185	.74	32.3	1000	30.95
1.0175	.46	20	400	20
1.023	.41	17.9	400	22.35
1.015	.15	6.5	100	15.4
1.025	.23	10	100	10
			6400	≈220 hours

TABLE V

Reaction (B): $e^+e^- \rightarrow \rho\pi \rightarrow \pi^+\pi^-\pi^o$; (D): $e^+e^- \rightarrow \pi\pi\eta$

Event type	Detection efficiency	(B)	(D)
1	Percentage of detected $\pi^+\pi^-$ (a), (b)	0.16	0.08
2	Percentage of detected $\pi^+\pi^-$, with both γ's of energy >0.1 GeV (a) (b)	0.013	0.03
3	Percentage of events of type 2 with γ detection efficiency as in (c)	0.008	0.019
	Number of detected events if a total of $4 \cdot 10^4$ reactions $e^+e^- \rightarrow \phi \rightarrow \rho\pi$ are produced		
4	Number of detected events of type 1 from the reaction B	6400	
5	Number of detected events of type 1 from reaction D assuming $(\phi \rightarrow \pi\pi\eta)/(\phi \rightarrow \rho\pi) = 0.01$		32
6	Number of detected events of type 3 from the reaction B	320	
7	Number of detected events of type 3 from the reaction D assuming $(\phi \rightarrow \pi\pi\eta)/(\phi \rightarrow \rho\pi) = 0.01$		8

(a) Efficiency of the experimental apparatus (counters and spark chambers) assumed to be 1.

(b) The losses due to nuclear interactions and range in the coil, are included

(c) γ detection efficiency in the external chambers is assumed to be 0.8 (1) (Shower electrons are visible at least in 3 bigaps)

TABLE VI

	$e^+e^- \to$	Observed channels	Decay frequency (See Tab.I,col.4)	Efficiency	$\sigma^{(13)}$	Events/hr$^{(*)}$	Events in 300 hr
1	$K^{*+}K^{*-}$	$K^o(\pi^+\pi^-)\pi^+\bar{K}^o(\pi^+\pi^-)\pi^-$ $K^o(\pi^+\pi^-)\pi^+K^-\pi^o$ $K^+\pi^o\bar{K}^o(\pi^+\pi^-)\pi^-$	0.2 0.3	detecting at least 5 charged prongs 0.23 detecting 4 charged prongs 0.13	5×10^{-33}	0.3	90
2	$K^{*o}\bar{K}^{*o}$	$K^-\pi^+K^+\pi^-$ $K^o(\pi^+\pi^-)\pi^oK^-\pi^+$ $K^+\pi^-\bar{K}^o(\pi^+\pi^-)\pi^o$	0.45 0.3	detecting at least 3 charged prongs 0.47 detecting 4 charged prongs 0.13	3×10^{-34}	0.06	18
3	$K^{*+}K^-$	$K^+\pi^oK^-$ $K^o(\pi^+\pi^-)\pi^+K^-$	0.33 0.45	detecting 2 charged prongs 0.36 detecting at least 3 charged prongs 0.47	10^{-36}	$0.24 10^{-3}$	1
4	$K^{*o}\bar{K}^o$	$K^o(\pi^+\pi^-)\pi^o\bar{K}^o(\pi^+\pi^-)$ $K^-\pi^+K^o(\pi^+\pi^-)$	0.15 0.45	detecting 4 charged prongs 0.13 detecting at least 3 charged prongs 0.47	3×10^{-33}	0.5	150
5	$\Phi\eta$	$K^+K^-\eta$ (neutrals)	$B(K^+K^-) = 0.48$ $B(\eta\to\text{neutrals})=0.71$	detecting 2 charged prongs 0.36	2×10^{-33}	0.18	54
6	$\rho^+\rho^-$	$\pi^+\pi^-(\pi^o,\pi^o)$		detecting 2 charged prongs 0.36	3.6×10^{-33}	2.6	780

(*) Nominal luminosity (16) at W = 2 GeV $L = 0.73\times10^{33}$ cm^{-2} h^{-1}

TABLE VII

Decay channels	Events in 400 hr
$K_L^o \to \pi^{\pm} e^{\mp} \nu$	3060
$\pi^{\pm} \mu^{\mp} \nu$	2360
$\pi^+ \pi^- \pi^o$	1020
($\pi^o \pi^o \pi^o$	1930)
$\pi^+ \pi^-$	14
$\pi^o \pi^o$	7 (assuming $\eta_{oo} = \eta_{+-}$)